
RANDOM ABSTRACT CELL COMPLEXES

A PREPRINT

Josef Hoppe*

Department of Computer Science
RWTH Aachen University
Aachen, Germany
hoppe@cs.rwth-aachen.de

Michael T. Schaub

Department of Computer Science
RWTH Aachen University
Aachen, Germany
schaub@cs.rwth-aachen.de

ABSTRACT

We define a model for random (abstract) cell complexes (CCs), similar to the well-known Erdős–Rényi model for graphs and its extensions for simplicial complexes. To build a random cell complex, we first draw from an Erdős–Rényi graph, and consecutively augment the graph with cells for each dimension with a specified probability. As the number of possible cells increases combinatorially — e.g., 2-cells can be represented as cycles, or permutations — we derive an approximate sampling algorithm for this model limited to two-dimensional abstract cell complexes. Since there is a large variance in the number of simple cycles on graphs drawn from the same configuration of ER, we also provide an efficient method to approximate that number, which is of independent interest. Moreover, it enables us to specify the expected number of 2-cells of each boundary length we want to sample. We provide some initial analysis into the properties of random CCs drawn from this model. We further showcase practical applications for our random CCs as null models, and in the context of (random) liftings of graphs to cell complexes. Both the sampling and cycle count estimation algorithms are available in the package `py-raccoon` on the Python Packaging Index.

Keywords Random Models · Null Models · Random Abstract Cell Complexes · Simple Cycles · Higher-Order Networks

1 Introduction

Since the seminal work of Erdős–Rényi [1], random models of relational data described by graphs have been a mainstay topic of interest within probability theory, statistics, data science and machine learning. The interest in such random graphs can be motivated from at least three perspectives. First, they are vital as generative models for complex networks in various disciplines, including social sciences, physics, and biology [2, 3], as they enable the theoretical and empirical study of how certain (random) connection mechanisms can influence the make-up of a network. Second, random models can serve as null models to evaluate whether some observed network statistics may be deemed significant. Third, random models can generate synthetic input data for training machine learning models, or for controlled experiments and benchmarking of network analysis algorithms.

Starting from the Erdős–Rényi (ER) model [1] and its variation by Gilbert [4] a vast array of models for random graphs has been developed, such as the Stochastic Block Model [5], the Configuration Model [6], etc. (see Appendix for more related literature). Many of these models allow for the direct or indirect specification of certain network statistics — e.g., density, triangle counts, degree distribution — to be preserved (either exactly or in expectation) in samples drawn from the model.

Recently, there has been a trend in studying higher-order network models such as hypergraphs and simplicial and cellular complexes [7, 8, 9]. These richer models for relational data have gained interest as they enable the study of complex network structures with interactions beyond pairwise relationships, which have been deemed to be essential to model certain systems. In contrast to random graph models, the landscape of models for these higher-order networks is however far less developed (see appendix for related work). In particular, even though (abstract) cell complexes feature

*<https://hoppe.io>

Evaluation Code and PyPI Package available at github.com/josefhoppe/random-abstract-cell-complexes.

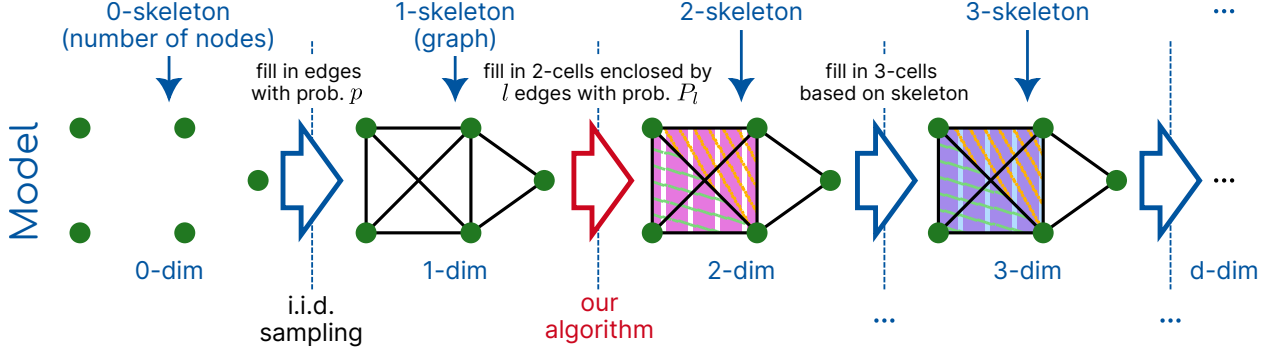


Figure 1: Overview of the random abstract cell complex model. The model is defined through iterative liftings from d to $d + 1$ -dimensional cell complexes. This makes it possible to fix a skeleton of the complex and only apply the random lifting for subsequent dimensions. In this paper, we focus on the lifting from one- to two-dimensional abstract cell complexes. For this, we present a novel, efficient approximate sampling algorithm (see Figure 2).

prominently in topological data analysis [10], and in the emerging area of topological signal processing [11, 12] and topological deep learning [13], there are hardly any models for random abstract cell complexes. Appendix A provides a more in-depth overview of related work.

Contributions. We define a model for random abstract cell complexes that generalizes the Linial-Meshulam model [14, 15] for SCs. Our model may also be used for random liftings of a given graph to a cell complex. We show that sampling from this model is non-trivial due to the combinatorial increase in the number of possible cells. Hence, we propose a novel algorithm to approximately sample from the model, focussing on two-dimensional abstract cell complexes. We provide an open source implementation of this algorithm in python. As a secondary result, our work results in an approximation algorithm to estimate the number of simple cycles in a graph, which may be of independent interest. Finally, we demonstrate the utility of our random cell complex model: we briefly analyze the orientability and homologies of sampled complexes; use it as a null model to create an evaluation baseline; and demonstrate the use of random liftings to gain insight to neural networks defined on cell complexes [16].

Outline. In the remainder of this paper, we first introduces relevant concepts and notation in Section 2 We then present our random cell complex model in Section 3 and introduce an efficient approximate sampling algorithm for two-dimensional abstract cell complexes in Section 4 . We analyze our algorithm both theoretically in Section 5 and empirically in Section 7. Finally, we provide some case studies on application of random CCs in Section 8.

2 Background and Notation

Graphs and simple cycles. We consider undirected graphs $G = (V, E)$ with $n := |V|$ nodes and $m := |E|$ edges. An Erdős–Rényi random graph $G(n, p)$ has n nodes and for any node pair $u, v \in V$, the edge (u, v) exists independently with probability p . A cycle c is a closed simple path on G ; its length $|c|$ equals the number of nodes (or edges) in c . We denote the set of all cycles in G by C . We use C_l to denote the set of all cycles $c \in C$ with length $|c| = l$ and $N_l = |C_l|$ to denote the number of cycles on a graph. If node u or edge (u, v) is part of the cycle c , we write $u \in c$ or $(u, v) \in c$, respectively.

Cycle bases and spanning trees. The cycle space of a graph is the set of its subgraphs in which every node has even degree. With addition defined as the symmetric difference and scalar multiplication with \mathbb{F}_2 , the cycle space is a vector space. A *cycle basis* is a set of *simple* cycles that is a basis of the cycle space. Any spanning tree T on a graph G induces a cycle basis [17]: Each edge (u, v) that is not in T closes the path from u to v on T , creating a simple cycle; the set of all induced cycles C_T is a cycle basis on G .

Uniform spanning trees and the Laplacian Random Walk. A uniform spanning tree is a spanning tree picked uniformly at random from all spanning trees on a given graph. Uniform spanning trees can be efficiently obtained by Wilson’s algorithm [18]. The probability of a certain path being included in a uniform spanning tree can be calculated via a particular absorbing random walk termed the Laplacian random walk [19].

3 A model for random abstract cell complexes

Random abstract cell complexes can be sampled through a series of iterative liftings, beginning with a set of n nodes and iteratively adding higher-dimensional cells. For two- and higher-dimensional cells, the number of possible cells depends on the size of the boundary (e.g. edges for 2-cells). Thus, for every dimension d and possible boundary size l , we define the inclusion probability $P_l^{(d)}$. Using these inclusion probabilities, we can now define our random cell complex model $\text{RCC}(n, P^{(1)}, \dots, P^{(d_{\max})})$, where the vector $P^{(i)} = (P_l^{(i)})$ collect the inclusion probabilities of i -cells with boundary size l . Each possible cell is added independently according to the inclusion probability (i.e., depending on the boundary size). For dimension $d = 2$ and above, the cells that can be added depend on the sampled cells from dimension $d - 1$. This iterative lifting-based model also allows us to augment any given CC with random higher-dimensional cells of specified dimensions.

Relationship to the Erdős–Rényi model. For 1-cells (edges), the only possible boundary size is 2. Therefore, the model $\text{RCC}(n, P^{(1)})$ is equal to $\text{ER}(n, P_2^{(1)})$.

Relationship to the Linial-Meshulam model. The RCC model can be seen as a generalization of the LM model. Specifically, to recover the LM model, we set $P_{d+1}^{(d)} = 1$ for all dimensions d except d_{\max} , resulting in a full simplicial complex. Then, by setting $P_{d_{\max}+1}^{(d_{\max})} = p$ and all other inclusion probabilities to 0, we obtain the LM model.

Properties of Random Cell Complexes Before continuing, we provide some empirical analysis on the properties of resulting cell complexes (obtained using the sampling algorithm introduced below). To improve interpretability, we discuss our results based on the number of sampled cells, rather than on the probability $P^{(2)}$. First, in Figure 18b, we can see that most obtained CCs are not orientable, even with relatively few added cells. Second, Figure 18a shows that in our experiments random CCs either have (almost) no 1-cohomology or (almost) no 2-cohomology. Qualitatively, these results also hold for CCs randomly generated from point cloud triangulations. However, these experiments are merely simple explorations performed with 1-skeletons drawn from the ER model with the same parameters. More research is needed to understand the behaviour of the RCC model in more detail, which is beyond the scope of the current work.

4 Sampling Algorithms for Lifting to two-dimensional CCs

As a step towards a sampling algorithm for the full model described above, we consider algorithms for the lifting from one-dimensional CCs (graphs) to two-dimensional CCs. As there is no risk of confusion in this context, we simply use P_l to refer to $P_l^{(2)}$ in the following.

4.1 Naïve sampling approaches

Rejection sampling for liftings of (nearly) complete graphs. A straightforward and exact approach to selecting appropriate cells is rejection sampling using random permutations of the nodes. More specifically, to sample a 2-cell with a boundary of length l , we draw permutations of the nodes with length l until we find a permutation that is a valid cycle on G . The rejection rate depends on the underlying graph. If we assume the graph to be sampled from ER, then one of p^{-l} permutations is a valid boundary of a 2-cell of length l , in expectation. Therefore, rejection sampling is well-suited only for sampling of short cells or on (almost) complete graphs, but too computationally complex in other cases.

Markov Chain Monte Carlo. MCMC algorithms sample from a probability distribution via random walks on all possible values, connected by a move set. A simple move set on simple cycles would be the symmetric difference with any set of simple cycles. However, this space may not be connected, e.g., on the graph of two triangles connected by an edge $\langle \blacktriangleright \blacktriangleleft \rangle$. Therefore, an MCMC algorithm would require a more complex move set, i.e., there is no trivial Markov chain Monte Carlo algorithm for sampling simple cycles.

4.2 An Approximate Algorithm for Lifting to two-dimensional abstract CCs

In this section, we introduce an efficient approximate sampling algorithm for random 2-cells. On a high level, the sampling algorithm works as depicted in Figure 2. It approximates sampling each cycle independently with a fixed target probability P_l from the (impractically large) set of all cycles in G with a two step sampling process. First, our algorithm samples s spanning trees T . Each of these trees results in a subset of induced cycles $C_T \subseteq C$. Note that every cycle c has a certain *occurrence probability* ρ_c to occur in such a set of cycles C_T . In the second step, the algorithm

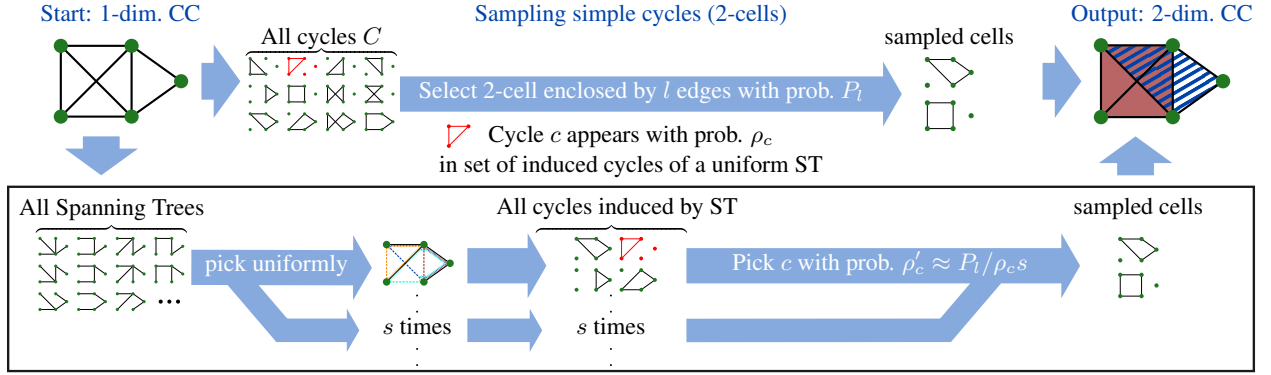


Figure 2: Random lifting from 1-dim. CC to 2-dim. CC and our sampling algorithm. The model (strong background colors) is simulated by dividing it into two steps (light background colors): First, s uniform spanning trees are sampled on the graph, each inducing a subset of all cycles. Depending on the probability ρ_c for any cycle to appear in such a subset, the cycles are then sampled as cells. The algorithm (boxes) closely follows the two-step sampling model, approximating ρ_c for efficiency.

selects cycles independently from these induced subsets, each with a specific probability ρ'_c that is calculated to obtain the desired target probability P_l .

Given the desired target sampling probability P_l , the occurrence probability ρ_c , and number of sampled trees s , we can calculate the selection probability ρ'_c as follows. Note, that each cycle c has an independent probability of $\rho_c \rho'_c$ to be selected from each of the s spanning trees. Hence we obtain the relationship:

$$P_l = 1 - (1 - \rho_c \rho'_c)^s \approx \rho_c \rho'_c s \quad \Leftrightarrow \quad \rho'_c = \frac{1 - \sqrt[s]{1 - P_l}}{\rho_c} \approx \frac{P_l}{\rho_c s} \quad (1)$$

We remark that the above equation only has a valid solution for $1 - \sqrt[s]{1 - P_l} < \rho_c$, i.e., only for sufficiently small target probabilities P_l or sufficiently large s . Otherwise, ρ'_c could become greater than 1. Since this occurs when the number of sampled trees is too low, we call this behavior *undersampling*. Also note that the sampled cells may be correlated, if we end up sampling multiple cells from the same spanning tree.

As the occurrence probability is still expensive to compute, we introduce two levels of approximations: a more accurate estimation denoted via tilde, and a less accurate estimation with two tildes. For example, ρ_c is approximated by $\tilde{\rho}_c$ or $\tilde{\tilde{\rho}}_c$, respectively. In line with our original RCC model, the approximation assumes that the graph was sampled from ER graph with (known) probability p . If the graph is given and p is not known, our approximation uses the maximum likelihood estimation $p \approx m / \binom{n}{2}$.

Probability ρ_c of cycles being induced by uniform spanning trees. To determine the selection probability ρ'_c in accordance with the target probability P_l , we have to estimate the occurrence probability ρ_c . Each cycle c is induced by a spanning tree if and only if it includes any path consisting of all but one edge of c . For each of these paths, we can calculate the probability of it being included in a uniform spanning tree via a so-called Laplacian Random Walk [19]. Since this walk is computationally expensive to calculate, we approximate the probability through multiple steps, most notably by approximating the 1-skeleton with the expected graph where each edge has weight p , and by approximating some node degrees with the expected degree. The full derivation of the formulae below can be found in Appendix C. We denote the degree of w by $d(w)$.

$$\tilde{\tau}_c^{(l-1)} = \frac{1}{1 + \frac{(d(w)-2) n-l}{n-3} \frac{n-l}{l}} \quad (2)$$

$$\tilde{\rho}_c = \frac{\sum_{(u,v) \in c} \tilde{\tau}_c^{(l-1)} (d(v)-1)(d(v')-1) \binom{n-2}{n}^{l-3} \frac{n-1}{n} \frac{(n-1)q-1}{(n-1)q}}{\prod_{w \in c} d(w)-1} \quad (3)$$

$$\tilde{\tilde{\rho}}_c = \frac{\sum_{(u,v) \in c} (d(v)-1)(d(v')-1) \binom{n-2}{n}^{l-3} \frac{n-1}{n} \frac{(n-1)q-1}{(n-1)q} \frac{1}{1 + \frac{(n-1)q-2}{n-3} \frac{n-l}{l}}}{\prod_{w \in c} d(w)-1} \quad (4)$$

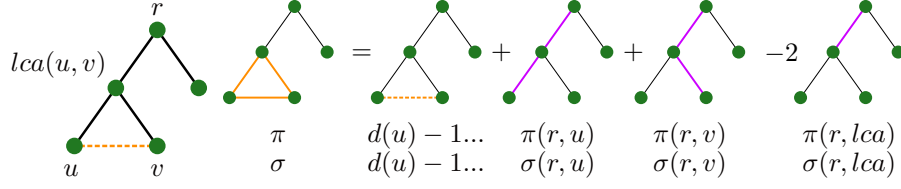


Figure 3: Illustration of the efficient calculation based on the tree structure.

5 Theoretical Considerations

In this section, we prove the algorithmic complexity of our sampling approach, discuss theoretical limitations of spanning-tree-based sampling, and show that a static configuration of our RCC model leads to heterogeneous two-dimensional CCs.

5.1 Algorithmic Complexity

Theorem 1. *On a connected 1-skeleton sampled from an ER model, our fast sampling approximation can be calculated in $\mathcal{O}(s \cdot m^{1+\varepsilon} + \ell)$, where ℓ is the sum of the lengths of the boundaries of all resulting cells.*

Proof. We can use Wilson’s Algorithm [18] to efficiently sample spanning trees. Wilson’s Algorithm is linear in the hitting time of the graph, i.e., the expected time a random walk from any node to any other node takes. In the worst case, the hitting time is $\mathcal{O}(n^3)$ [20]. However, we are assuming the graph to be sampled from an ER model with probability p such that the resulting graph is almost surely connected as the number of nodes becomes large ($n \rightarrow \infty$). On these ER-Graphs, the hitting time is in $\mathcal{O}(n)$ [21].

First, we decompose $\tilde{\rho}_c$ into three components: The sum component $\sigma = \sum_{(u,v) \in c} \dots$, the product component $\pi = \prod_{w \in c} \dots$, and the remaining component $\gamma(n, p, l)$, such that $\tilde{\rho}_c = \sigma \cdot \gamma(n, p, l) / \pi$. Instead of calculating the two components π, σ over each cycle, we utilize the spanning tree structure as illustrated in Figure 3: Given a spanning tree, we choose an arbitrary root r . We define the components as $\sigma(u, v)$ ($\pi(u, v)$) over the path from u to v . For the empty path, we define $\pi(r, r) = d(r) - 1, \sigma(r, r) = 0$. For a node u with parent v , we calculate $\pi(r, u) = \pi(r, v) \cdot (d(u) - 1)$ and $\sigma(r, u) = \sigma(r, v) + (d(v) - 1)(d(u) - 1)$. For any nodes u, v :

$$\pi(u, v) = \frac{\pi(r, u)\pi(r, v)(d(\text{lca}(u, v)) - 1)}{\pi(r, \text{lca}(u, v))^2} \quad (5)$$

$$\sigma(u, v) = \sigma(r, u) + \sigma(r, v) - 2\sigma(r, \text{lca}(u, v)) + (d(v) - 1)(d(u) - 1) \quad (6)$$

This only covers the path, thus we close the cycle: $\pi = (d(u) - 1)(d(v) - 1)\pi(u, v)$ and $\sigma = (d(u) - 1)(d(v) - 1) + \sigma(u, v)$, respectively. Both components take $\mathcal{O}(n) \leq \mathcal{O}(m)$ to calculate per tree. For a more detailed example on a toy graph, see Appendix B.

To compute the lowest common ancestor (lca) of two nodes, we use Tarjan’s off-line lca algorithm [22], which runs in $\mathcal{O}(n + m\alpha(n + m))$ (per tree), where α is the inverse of the Ackermann function. On a connected graph, the number of edges is, asymptotically, at least as large as the number of nodes, i.e., we can simplify the complexity of lca to $\mathcal{O}(m\alpha(m)) \leq \mathcal{O}(m^{1+\varepsilon})$ for any $\varepsilon > 0$.

Note that we only need to completely enumerate the cells that are sampled. When a cell is selected, we take the two nodes it is induced by and walk from each to their lowest common ancestor, thus obtaining the boundary; and taking $\Theta(\ell)$ steps over all spanning trees.

The theorem follows from the sum of these complexities. \square

For the non-approximated estimation, it takes $\mathcal{O}(s \cdot m \cdot l) \leq \mathcal{O}(s \cdot m \cdot n)$, where l is the average length of occurring cycles, to calculate the probabilities instead. In contrast, calculating ρ_c exactly needs at least $\Omega(sm n^2)$.

5.2 Theoretical Limitations

Before investigating the accuracy of our estimation approach in practice, we consider some theoretical limitations of spanning-tree-based cycle sampling.

To this end, let us consider the complete graph K_n , on which the prior estimation of the number of cycles \mathcal{N}_l and our approximated occurrence probability $\tilde{\rho}_c$ are exact. Overall, longer cycles are less frequently induced by a spanning tree (compare Figure 5a), since the probability of any cycle being induced converges faster to zero than the number of possible cycles grows. As we will see later, this also holds for smaller values of p .

Overcoming this would require an impractically large number of samples. In the worst case, the expected number of sampled cells c with length $l = n$ in one spanning tree is:

$$N_l \rho_c = \frac{n!}{(n-n)!} \frac{1}{2l} \cdot \frac{l}{1 + \frac{n-l}{n}} \frac{(n-2)^2}{n^{n-2}} = \frac{n!}{2} \frac{(n-2)^2}{n^{n-2}} \quad (7)$$

In other words, we would need to sample $\frac{1}{N_l \rho_c} \approx 2.2 \cdot 10^{34}$ spanning trees to get a single cycle for $n = l = 100$ in expectation.

5.3 Heterogeneity for static target probability P_l

With a fixed probability P_l for each possible cell to be sampled, given the same parameter configuration, some sampled CCs will have ten times the expected 2-cells while others have none. We can estimate the number of cells from the a priori estimation of the number of simple cycles \mathcal{N}_l and the target probability P_l . However, as Figure 9 shows, there is a large variance in the correct count N_l , which translates to a similar variance in the number of cells. For practical applications, this behavior may be important to consider. If required, this behavior can be changed by adjusting $P^{(2)}$ based on the realization of the 1-skeleton. However, while the total number of edges in a graph is easy to calculate, the total number of simple cycles is not.

6 Obtaining more homogenous cell complex configurations based on cycle count estimation

In practical applications, the large heterogeneity in the number of 2-cells arising from a fixed P_l can be a problem. For a graph with N_l cycles of length l , we expect a total of $P_l \cdot N_l$ 2-cells. Given the number of cycles N_l , we could therefore adjust P_l to result in a desired number of 2-cells with boundary length l (in expectation). However, in contrast to the number of edges, the number of cycles N_l is not trivial to compute for an arbitrary length l [23] and accurate methods are computationally inefficient. Therefore, we introduce an approximation algorithm that works similar to our sampling algorithm: We estimate the number of cycles with length l by simulating sampling from s spanning trees with $P_l = 1$. In contrast to actual sampling, we do not explicitly identify all induced cycles. Therefore, a cycle that occurs in multiple sampled spanning trees will also be counted multiple times. Thus, to achieve a desired probability P_l to count cells, we introduce the counting coefficient ρ_c'' :

$$P_l = \rho_c \rho_c'' s \Rightarrow \rho_c'' = \frac{P_l}{\rho_c s} = \frac{1}{\rho_c s} \quad \text{for } P_l = 1 \quad (8)$$

Below, we motivate that the sum counting coefficients ρ_c'' of induced cycles approximates the count of all cycles N_l : $N_l \approx \sum_T \sum_{c \in C_l \cap C_T} \rho_c''$.

Given a graph G , let \mathbb{T} be the set of all spanning trees of G and $\mathbb{T}_c := \{T \in \mathbb{T} : c \in C_T\}$ the set of all spanning trees that induce a given cycle c . Note that the occurrence probability ρ_c of a cycle c can be expressed in terms of the cardinalities of these sets of spanning trees, i.e., $\rho_c = |\mathbb{T}_c|/|\mathbb{T}|$. In the ideal case, where we iterate over all trees \mathbb{T} and the number of samples $s = |\mathbb{T}|$ is the number of all spanning trees, this accurately counts all cycles:

$$N_l = \sum_{c \in C_l} 1 = \sum_{c \in C_l} \sum_{T \in \mathbb{T}_c} \frac{1}{|\mathbb{T}_c|} = \sum_{T \in \mathbb{T}} \sum_{c \in C_l \cap C_T} \frac{1}{|\mathbb{T}_c|} = \sum_{T \in \mathbb{T}} \sum_{c \in C_l \cap C_T} \frac{1}{\rho_c |\mathbb{T}|} = \sum_{T \in \mathbb{T}} \sum_{c \in C_l \cap C_T} \rho_c'' \quad (9)$$

In practice, we effectively approximate \mathbb{T} with uniformly sampled spanning trees T_1, \dots, T_s for a relatively small number of samples $s \ll |\mathbb{T}|$. Practical numbers of samples s tend to result in counting coefficients ρ_c'' that are greater than 1. Summing these counting coefficients ρ_c'' of all induced cycles results in the desired approximation:

$$N_l \stackrel{(9)}{=} \sum_{T \in \mathbb{T}} \sum_{c \in C_l \cap C_T} \frac{1}{\rho_c |\mathbb{T}|} \approx \frac{|\mathbb{T}|}{s} \sum_{i=1}^s \sum_{c \in C_l \cap C_{T_i}} \frac{1}{\rho_c |\mathbb{T}|} = \sum_{i=1}^s \sum_{c \in C_l \cap C_{T_i}} \frac{|\mathbb{T}|}{s} \cdot \frac{1}{\rho_c |\mathbb{T}|} = \sum_{i=1}^s \sum_{c \in C_l \cap C_{T_i}} \rho_c'' \quad (10)$$

An alternative interpretation based on individual cycles is illustrated in Figure 4: Given a spanning tree T , we can use the induced cycles C_T and their occurrence probabilities to estimate the total number of cycles on the graph: First, we

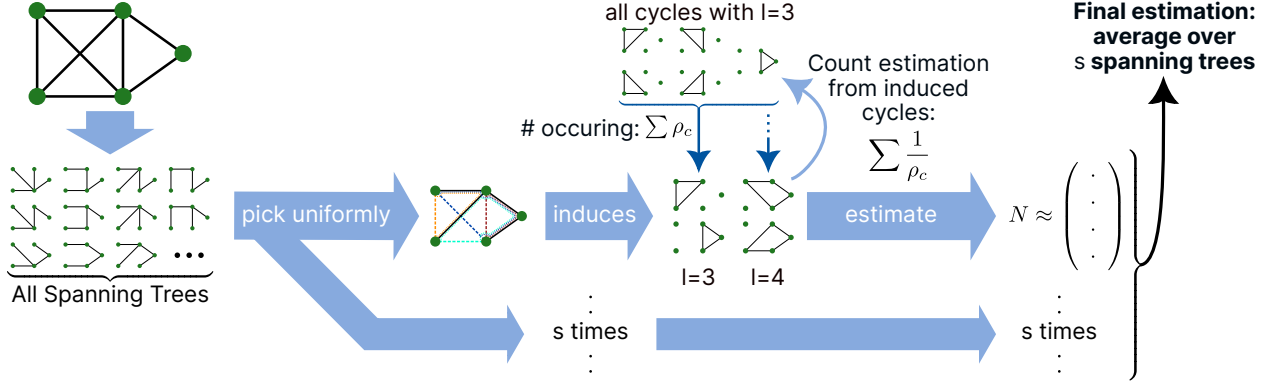


Figure 4: The cycle count estimation uses the same basic structure as the sampling algorithm. The occurring cycles and their occurrence probabilities can be used to estimate the total number of cycles: The expected number of induced cycles with length l is the sum of the occurrence probabilities of all such cycles. To estimate the total number, we can invert this idea: For every occurring cycle c there are (approximately speaking) $1/\rho_c$ cycles with the same occurrence probability: This results in sampling, in expectation, $\rho_c \cdot 1/\rho_c = 1$ occurring cycle. The approach, again, samples s spanning trees, taking the average cycle count estimation.

assume that the occurrence probabilities ρ_c of the induced cycles are representative of all occurrence probabilities of cycles of the same length. Second, on average, if a cycle c of length l occurs with probability ρ_c , there are $1/\rho_c$ cycles with that length. Finally, to improve the accuracy of this estimate, we average the result over s spanning trees.

Note that the accuracy of the estimation depends on how accurately the occurring cycles represent the distribution of cycles (with regard to both the cycle lengths and occurrence probabilities) induced by spanning trees. With sufficiently many samples, the law of large numbers says that the cycles will be representative, i.e., the estimate will be accurate. It is unclear how to determine the number of samples required for the approximation to become accurate. However, the number of induced cycles of each length can serve as an indicator: If there are only few or even a single induced cycle for a certain length l , we don't have confidence in the estimated number N_l . Thus, we also count the number of occurrences $o_l = \sum_{T_i} |C_l \cap C_{T_i}|$.

Sampling with expected number of cells To ensure a sufficiently accurate estimation of N_l , we only sample cells with boundary lengths $L := \{3 \leq l \leq n : o_l > t\}$ that occur more often than a user-specified threshold t . Calculating P_l to achieve any desired number in expectation is now simple; if desired, one can also distribute an overall number evenly over all occurring lengths. In this paper, we use ν to denote an expected number of cells evenly distributed among occurring lengths.

7 Empirical Evaluation of the Sampling Algorithm

The evaluation code is available under github.com/josefhoppe/random-abstract-cell-complexes.

7.1 Sampling Accuracy

First, we compare our approximations to estimate the occurrence probability $\tilde{\rho}_c$. We evaluate this by first sampling a single graph from an ER model, then sampling multiple spanning trees, and calculating the ρ_s for all cycles induced by the spanning trees.

Figure 6 shows that, given a sufficiently large number of nodes n and connection probability p , both approximations of ρ are very accurate. However, as Figure 10 shows, that for graphs that are relatively sparse the accuracy drops. This is likely a result of graphs with smaller edge probabilities behaving more differently from the expected graph: Our approximation assumes a relatively densely and evenly connected graph. Sparse configurations of ER are more likely to deviate from this expectation than dense configurations: The degree distribution is less uniform and a path is more likely to 'cut off' parts of the graph due to the lower connectivity.

On graphs that are not densely and evenly connected, our approximation still utilizes the degree of nodes on the induced cycles, providing some accuracy. A comparison with Figure 11 shows that, on both sparse and dense graphs, our approximation is much more accurate than assigning each cycle the average probability of all cycles with the same length.

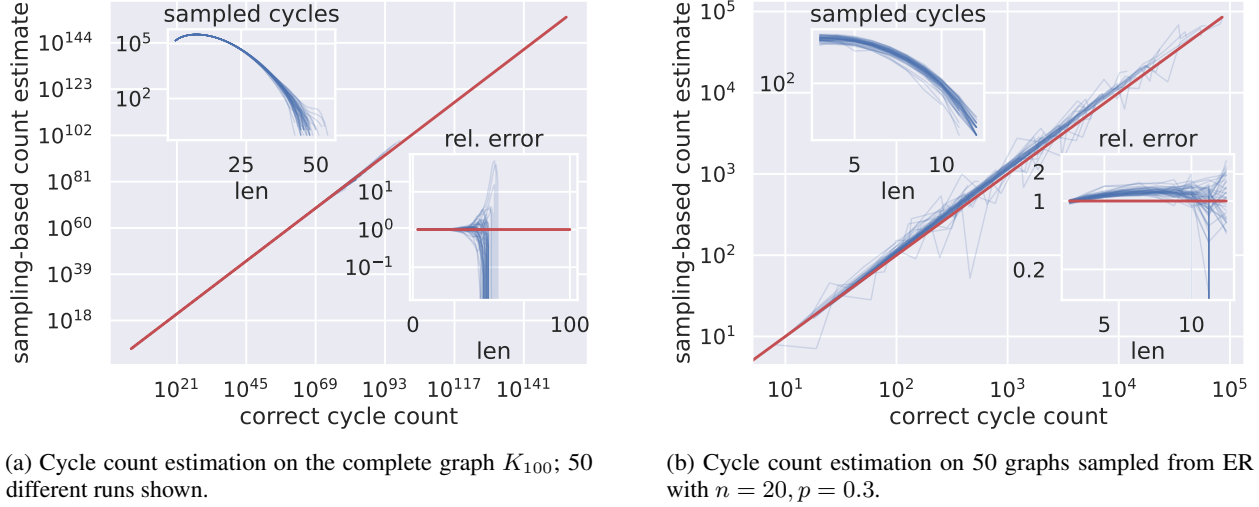


Figure 5: The cycle count estimation \tilde{N}_l and the actual number of cycles N_l (red). With increasing l , cycles become less likely to be induced by a spanning tree. This results in a lower accuracy and estimates of $\tilde{N}_l = 0$ for larger l .

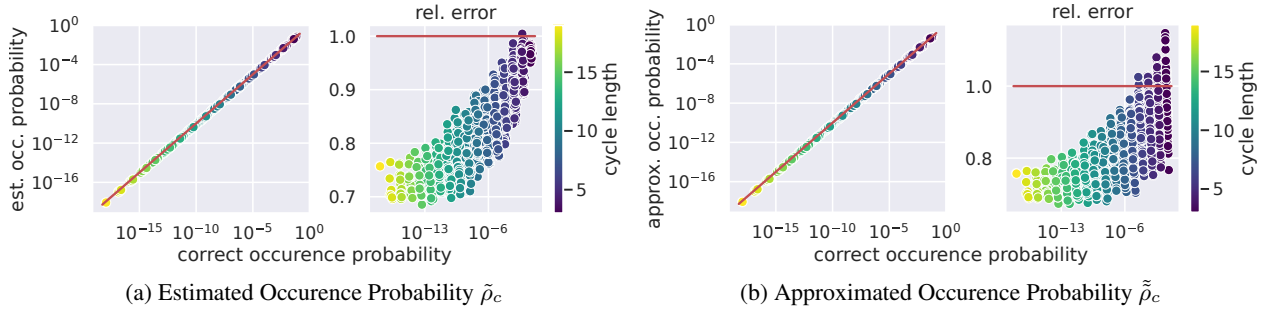


Figure 6: The estimated (a) and approximated (b) occurrence probability of simple cycles on one graph sampled from ER with $n = 30, p = 0.5$; cycles for evaluation obtained from 10 uniform STs. Both methods are very close to the correct probabilities. Especially for shorter cycles, the estimated probability is more accurate. This is to be expected, as for longer cells, the relative variance is naturally smaller and the likelihood of the last step is less dependent on the degree.

We evaluate the accuracy of the cycle count estimation by also calculating the correct number of cycles. For ER-Graphs, this means we have to choose small instances to sample from, making it possible to enumerate all cycles. Additionally, on the full graph, we can easily calculate the number of simple cycles, making it suitable for a comparison of the performance on larger graphs.

Given the good accuracy of the occurrence probability approximation, we expect the cycle count estimation to be similarly accurate, with the added condition that sufficiently many cells of the given length were induced by the sampled spanning trees. Figure 5b confirms this expectation, showing a slight overestimation for smaller lengths and a large increase in the error for longer cells. Furthermore, our experiments on the full graph (Figure 5a) show that the increase in error for longer cells is a result of the small number of sampled cycles since, on the full graph, all cells are the same and the estimated probability is always correct. This is exactly in line with our theoretical considerations.

Overall, the sampled number of cells that is very close to the desired number, as shown in Figure 17. Note that any skew of the occurrence probability results in an equal but opposite skew in the estimated number of cycles, leading in total to an accurate number of cells sampled.

7.2 Accuracy of random liftings on non-ER graphs

Our general random cell complex model can also be used to describe random cell complexes with a fixed d -skeleton. Our sampling algorithm can therefore be leveraged to provide a random lifting of any graph to a two-dimensional cell

complex. However, given that our approximations used in the sampling procedure are based on the assumption that the graph was sampled from ER, we expect a lower accuracy.

Figure 12a shows the estimation accuracy on a graph sampled from a homophilic configuration of the SBM. Interestingly, the overall accuracy is still quite close to the accuracy on ER graphs. In fact, this pattern also holds for heterophilic graphs, shown in Figure 12b. Our findings extend even to the case of a complete bipartite graph, although, as Figure 14 shows, we do see a small but consistent overestimation of the number of cycles. Furthermore, the approximated occurrence probability ρ_c is surprisingly good in both cases (cf Figure 13).

So far, we have only evaluated our algorithm on graph models that have regular shapes, with all nodes symmetric in expectation. Figure 15 shows the result on graphs sampled from the Barabasi-Albert model and a Configuration model with an uneven degree distribution. The accuracy is comparable to the accuracy on graphs sampled from the SBM, i.e., still higher than expected.

Overall, in our experiments, any deviation from an evenly and densely connected graph reduces the accuracy of our estimation: Communities, overall low connectivity, or uneven degree sequences make the estimation less accurate. Therefore, we expect a similar behavior on real-world graphs: It should work well on graphs with relatively evenly distributed degrees that are evenly and densely connected. Figure 16 shows that our experiments are in line with this expectation: Zachary’s Karate Club, which famously consists of two communities, is estimated less accurately than the November 17 network, which also has a higher average node degree.

7.3 Time complexity

Figure 7 shows that our approach is highly scalable. In configurations where the approximated occurrence probability is worse, the estimated is also relatively efficient. Empirically, the runtimes for both approaches are in line with our analysis: The slower estimation takes approximately $\mathcal{O}(n^{2.6})$; the faster approximation takes approximately $\mathcal{O}(n^2)$, which is consistent with $\mathcal{O}(s \cdot m^{1+\varepsilon})$ since $m \in \Theta(n^2)$ for a fixed p .

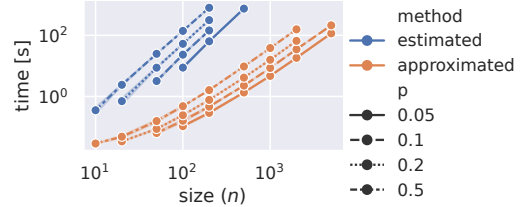


Figure 7: Runtime for $\nu = 10n$, $s = 1000$.

8 Applications

In this section, we explore the use cases for random cell complexes we identified earlier. We focus on minimal examples showcasing the usage rather than a comprehensive analysis.

8.1 Null Model as Experiment Baseline

When evaluating novel methods that infer cells, it is useful to have a baseline that marks randomness. In the case of the flow representation learning problem [24], we see that random 2-cells are very inefficient in Figure 8. However, this also gives us a way to classify the performance of the approaches we want to evaluate. In this case, we see that the newly proposed methods give a representation that provides a significant improvement over *triangles*, but *triangles* is already a method that explains a lot of structure.

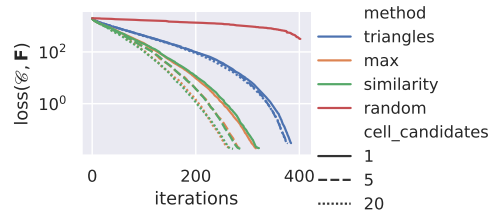


Figure 8: Comparison of the approaches to the flow representation learning problem from [24] and using random CCs (Anaheim dataset [25])¹.

8.2 Sensitivity analysis: how important are higher-order interactions?

In this section, we demonstrate the use of random CCs for the sensitivity (or ablation analysis [26]) of neural networks defined on higher-order networks.

In [16], Bodnar et al. propose a novel architecture for cell complex neural networks (CWNs). To obtain a cell complex and capture structural information on a graph, they add chordless cycles as 2-cells. On the synthetic *RingTransfer* benchmark, the authors demonstrate that 2-cells also improve the propagation of node features. Here we use our random cell complex model to investigate in how far this specific choice of 2-cells is relevant or if adding random cells would

¹Code available at github.com/josephoppe/random-abstract-cell-complexes.

have yielded similar results. This provides insights into whether it is the *specific* cell structure (adding chordless cycles) that conveys an advantage, or whether it is merely the increase in expressive power of the neural networks (resulting from adding higher-order cells) that is of importance.

Interestingly, for the PROTEINS dataset (see Table 1) there is no significant performance difference if we simply add random 2-cells instead of following the procedure outlined in [16]. Indeed, a similar performance can even be gained by not adding any 2-cells at all. In contrast, on the NCI109 dataset [27], adding random 2-cells significantly decrease the accuracy. This observation indicates that the 2-cell lifting procedure proposed in [16] works as intended on NCI109, but fails to capture relevant topological information on PROTEINS beyond what we could expect by simply increasing the expressivity of the network. To corroborate our findings, we have added a further comparison to the PPGN architecture [28]. PPGN also features an increased expressivity compared to standard GNNs, but is not based on any topological considerations. As Table 1 shows PPGN works well in the PROTEIN dataset, yet only performs as good as adding random cells in CWN. In conclusion, this example hints at how random cell complexes can lead to further insights into what features drive the performance of higher-order GNNs.

Table 1: Comparison of CWN [16] with the original 2-cells ('Rings'), random 2-cells ('RND'), and no 2-cells ('None'). Code available at github.com/josefhoppe/cwn-random-ccs. Results deviate slightly from [16] despite using the original code. Accuracy of PPGNs from [16].

DATASET [27]	PROTEINS	NCI109
CWN (RINGS)	73.8 ± 4.3	84.5 ± 1.6
CWN (RND)	74.2 ± 5.0	82.2 ± 1.3
CWN (NONE)	73.0 ± 5.5	82.9 ± 1.2
PPGNs [28]	77.2 ± 4.7	82.2 ± 1.4

9 Conclusion

The main contributions of this paper are (i) the introduction of a simple model for random abstract cell complexes, (ii) an efficient approximate sampling algorithm for this model, and (iii) a cycle count estimation algorithm required to make the model more amenable to application scenarios, in which we want to fix the number of certain cells in expectation. We explored some properties of this model and showcased how it enables a number of investigations concerning higher-order network data and learning methods operating with such data: Specifically, random CCs can be used as synthetic input data and as null models for multiple purposes.

This groundwork opens up multiple avenues for future research on abstract cell complexes: First, a more theoretical analysis of the number of simple cycles and the behavior of RCCs. Second, while we defined our model for arbitrary dimensions, higher-dimensional cells add considerable combinatorial complexity, which is why we limited our sampling algorithm to 2-cells. Indeed, adapting our sampling algorithm to higher-order cells is not trivial as the higher-dimensional analogues of spanning trees do not share many of their desirable properties.

When employing random cell complexes as synthetic data, it may also be desirable to include more structure in the cell complexes, both on the edge and cell levels. On the level of 2-cells, a simple extension could introduce a block structure and modify the sampling probabilities based on block membership.

Finally, the cycle count estimation is useful in its own right. To ensure it is suitable for the task, future work should evaluate its accuracy and compare it further to previous approaches, which is out of scope for this paper.

Acknowledgements

Funded by the European Union (ERC, HIGH-HOPeS, 101039827). Views and opinions expressed are however those of the author(s) only and do not necessarily reflect those of the European Union or the European Research Council Executive Agency. Neither the European Union nor the granting authority can be held responsible for them.

References

- [1] Paul Erdős and Alfréd Rényi, "On random graphs I," *Publ. math. debrecen*, vol. 6, no. 290-297, pp. 18, 1959.
- [2] Réka Albert and Albert-László Barabási, "Statistical mechanics of complex networks," *Reviews of modern physics*, vol. 74, no. 1, pp. 47, 2002.
- [3] Mikhail Drobyshvskiy and Denis Turdakov, "Random graph modeling: A survey of the concepts," *ACM computing surveys (CSUR)*, vol. 52, no. 6, pp. 1–36, 2019.
- [4] Edgar N Gilbert, "Random graphs," *The Annals of Mathematical Statistics*, vol. 30, no. 4, pp. 1141–1144, 1959.

- [5] Paul W Holland, Kathryn Blackmond Laskey, and Samuel Leinhardt, “Stochastic blockmodels: First steps,” *Social networks*, vol. 5, no. 2, pp. 109–137, 1983.
- [6] Bailey K Fosdick, Daniel B Larremore, Joel Nishimura, and Johan Ugander, “Configuring random graph models with fixed degree sequences,” *Siam Review*, vol. 60, no. 2, pp. 315–355, 2018.
- [7] Christian Bick, Elizabeth Gross, Heather A Harrington, and Michael T Schaub, “What are higher-order networks?,” *SIAM Review*, vol. 65, no. 3, pp. 686–731, 2023.
- [8] Leo Torres, Ann S Blevins, Danielle Bassett, and Tina Eliassi-Rad, “The why, how, and when of representations for complex systems,” *SIAM Review*, vol. 63, no. 3, pp. 435–485, 2021.
- [9] Federico Battiston, Giulia Cencetti, Iacopo Iacopini, Vito Latora, Maxime Lucas, Alice Patania, Jean-Gabriel Young, and Giovanni Petri, “Networks beyond pairwise interactions: Structure and dynamics,” *Physics Reports*, vol. 874, pp. 1–92, 2020.
- [10] Larry Wasserman, “Topological data analysis,” *Annual Review of Statistics and Its Application*, vol. 5, pp. 501–532, 2018.
- [11] Sergio Barbarossa and Stefania Sardellitti, “Topological signal processing over simplicial complexes,” *IEEE Transactions on Signal Processing*, vol. 68, pp. 2992–3007, 2020.
- [12] Michael T Schaub, Yu Zhu, Jean-Baptiste Seby, T Mitchell Roddenberry, and Santiago Segarra, “Signal processing on higher-order networks: Livin’ on the edge... and beyond,” *Signal Processing*, vol. 187, pp. 108149, 2021.
- [13] Mustafa Hajij, Ghada Zamzmi, Theodore Papamarkou, Nina Miolane, Aldo Guzmán-Sáenz, Karthikeyan Natesan Ramamurthy, Tolga Birdal, Tamal K Dey, Soham Mukherjee, Shreyas N Samaga, et al., “Topological deep learning: Going beyond graph data,” *arXiv preprint arXiv:2206.00606*, 2022.
- [14] Nathan Linial* and Roy Meshulam*, “Homological connectivity of random 2-complexes,” *Combinatorica*, vol. 26, no. 4, pp. 475–487, 2006.
- [15] Armindo Costa and Michael Farber, “Random simplicial complexes,” in *Configuration Spaces: Geometry, Topology and Representation Theory*, pp. 129–153. Springer, 2016.
- [16] Cristian Bodnar, Fabrizio Frasca, Nina Otter, Yuguang Wang, Pietro Lio, Guido F Montufar, and Michael Bronstein, “Weisfeiler and lehman go cellular: Cw networks,” *Advances in Neural Information Processing Systems*, vol. 34, pp. 2625–2640, 2021.
- [17] Maciej Marek Sysło, “On cycle bases of a graph,” *Networks*, vol. 9, no. 2, pp. 123–132, 1979.
- [18] David Bruce Wilson, “Generating random spanning trees more quickly than the cover time,” in *Proceedings of the twenty-eighth annual ACM symposium on Theory of computing*, 1996, pp. 296–303.
- [19] JW Lyklema, Carl Everts, and L Pietronero, “The laplacian random walk,” *Europhysics Letters*, vol. 2, no. 2, pp. 77, 1986.
- [20] Graham Brightwell and Peter Winkler, “Maximum hitting time for random walks on graphs,” *Random Structures & Algorithms*, vol. 1, no. 3, pp. 263–276, 1990.
- [21] Matthias Löwe and Felipe Torres, “On hitting times for a simple random walk on dense erdős–rényi random graphs,” *Statistics & Probability Letters*, vol. 89, pp. 81–88, 2014.
- [22] Robert Endre Tarjan, “Applications of path compression on balanced trees,” *Journal of the ACM (JACM)*, vol. 26, no. 4, pp. 690–715, 1979.
- [23] Pierre-Louis Giscard, Nils Kriege, and Richard C Wilson, “A general purpose algorithm for counting simple cycles and simple paths of any length,” *Algorithmica*, vol. 81, pp. 2716–2737, 2019.
- [24] Josef Hoppe and Michael T Schaub, “Representing edge flows on graphs via sparse cell complexes,” in *The Second Learning on Graphs Conference*, 2023.
- [25] Transportation Networks for Research Core Team, “Transportation networks for research,” 2020, Accessed: 2024-01-29.
- [26] Chris Fawcett and Holger H Hoos, “Analysing differences between algorithm configurations through ablation,” *Journal of Heuristics*, vol. 22, pp. 431–458, 2016.
- [27] Christopher Morris, Nils M Kriege, Franka Bause, Kristian Kersting, Petra Mutzel, and Marion Neumann, “TUDataset: A collection of benchmark datasets for learning with graphs,” *arXiv preprint arXiv:2007.08663*, 2020.
- [28] Haggai Maron, Heli Ben-Hamu, Hadar Serviansky, and Yaron Lipman, “Provably powerful graph networks,” *Advances in neural information processing systems*, vol. 32, 2019.

-
- [29] Pim van der Hoorn, Gabor Lippner, and Dmitri Krioukov, “Sparse maximum-entropy random graphs with a given power-law degree distribution,” *Journal of Statistical Physics*, vol. 173, pp. 806–844, 2018.
- [30] Duncan J Watts and Steven H Strogatz, “Collective dynamics of ‘small-world’ networks,” *nature*, vol. 393, no. 6684, pp. 440–442, 1998.
- [31] Jesper Dall and Michael Christensen, “Random geometric graphs,” *Physical review E*, vol. 66, no. 1, pp. 016121, 2002.
- [32] Matthew Kahle, “Topology of random clique complexes,” *Discrete mathematics*, vol. 309, no. 6, pp. 1658–1671, 2009.
- [33] Matthew Kahle et al., “Topology of random simplicial complexes: a survey,” *AMS Contemp. Math*, vol. 620, pp. 201–222, 2014.
- [34] Martina Zähle, “Random cell complexes and generalised sets,” *The Annals of Probability*, pp. 1742–1766, 1988.
- [35] Benjamin Schweinhart, Jeremy K Mason, and Robert D MacPherson, “Topological similarity of random cell complexes and applications,” *Physical Review E*, vol. 93, no. 6, pp. 062111, 2016.
- [36] Lutz Leistritz and Martina Zähle, “Topological mean value relations for random cell complexes,” *Mathematische Nachrichten*, vol. 155, no. 1, pp. 57–72, 1992.
- [37] Chris Whong, “FOILing nyc’s taxi trip data,” 2014, https://chriswhong.com/open-data/foil_nyc_taxi/. Last Accessed 2024-03-28.
- [38] Stefania Sardellitti, Sergio Barbarossa, and Lucia Testa, “Topological signal processing over cell complexes,” in *2021 55th Asilomar Conference on Signals, Systems, and Computers*. IEEE, 2021, pp. 1558–1562.
- [39] Oded Schramm, “Scaling limits of loop-erased random walks and uniform spanning trees,” *Israel Journal of Mathematics*, vol. 118, no. 1, pp. 221–288, 2000.
- [40] Wayne W Zachary, “An information flow model for conflict and fission in small groups,” *Journal of anthropological research*, vol. 33, no. 4, pp. 452–473, 1977.
- [41] CJ Rhodes and P Jones, “Inferring missing links in partially observed social networks,” *Journal of the operational research society*, vol. 60, no. 10, pp. 1373–1383, 2009.

A Related Work

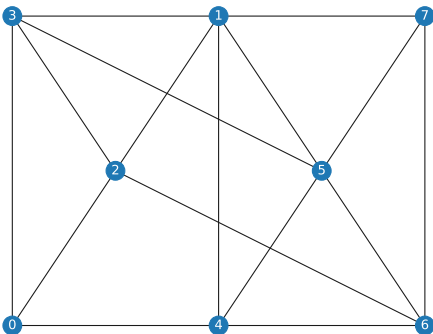
Random graph models. Random graph models started with the Erdős–Rényi random graph model [1], which originally proposed to draw a graph uniformly at random from the set of all graphs with a fixed number of nodes and edges. In this paper, we refer to a variant introduced by Gilbert [4] but commonly also referred to as Erdős–Rényi model, that draws each edge independently with probability p . More complex graph models generally focus on modeling community structure (most notably the Stochastic Block Model [5]) or the distribution of node degrees [2, 29]. Furthermore, there are models aimed to more closely approximate real-world networks, such as the Watts-Strogatz small-world graph [30], modeling the small diameter of real-world networks. Finally, graphs may be generated from random point clouds by connecting nodes that are close to each other in metric space [31]; resulting in the formation of clusters similar to real-world networks. There are many more models and ways to configure models that would exceed the scope of this literature review, but it should be noted that many use cases for these models exist, requiring different graph models.

Random simplicial complex models. The Linial-Meshulam model for random SCs [14] is an extension of Erdős–Rényi to higher dimensions. LM takes a complete $(d-1)$ -dimensional complex and samples i.i.d. from all possible d -simplices. The Linial-Meshulam model was generalized in multiple ways, e.g. a different static probability P_d to sample d -simplices (separately) for each dimension (i.e., cardinality) d [15]. In a similar vein to our model, random clique complexes [32], i.e., SCs obtained by adding all cliques of a random graph as simplices, build on a graph as a 1-skeleton. We refer to [33, 15] for a more detailed overview of existing models. To date, no SC model analogues to many of the well-known random graph models (e.g. modeling community structure, degree distribution, etc.) exist.

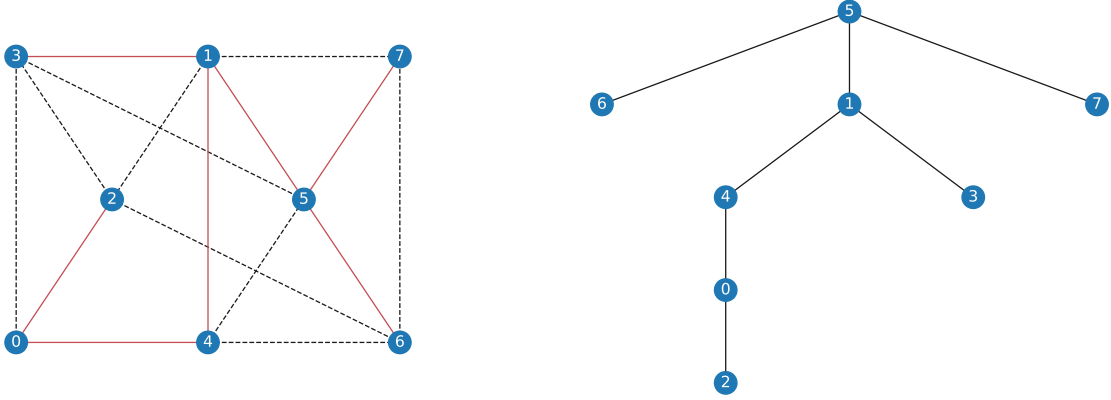
Random (abstract or geometric) cell complex models. On a theoretical level, random cell complexes in high-dimensional euclidean spaces were introduced by [34]. This results in geometric cell complexes, i.e., cell complexes that have an embedding and a distinction between cells that lie on the inside of the complex and those on the outside. Moreover, to the best of our knowledge, there is no known efficient algorithm to sample from this distribution. Further research on random geometric cell complexes [35, 36] focused on tessellations of low- or high-dimensional point clouds and the local topology characterizing physical cell complexes. Such geometric graphs (or CCs) may accurately model some real-world datasets (e.g., communication between internet nodes) as they result in sparse, planar graphs with a possibly quite large diameter. However, many applications have more dense, non-planar graphs with small diameters, such as telecommunication between cell towers [11], taxi trips (by endpoints) between neighborhoods [37], or social networks. To date, researchers have filled the gaps in both models and sampling algorithms for existing models by using simple lifting procedures, lifting a well-structured graph to an abstract cell complex, or using a possibly biased sampling method. Limiting the lifting to chordless cycles up to a certain length, for example, makes it computationally feasible to compute all possible 2-cells (in practice) [16]. Alternatively, cells can be sampled from the Delaunay triangulation of a two-dimensional point cloud [24, 38]. However, these are ad hoc constructions to provide a useful lifting for certain datasets or synthetic data for an evaluation, respectively. These methods have geometric properties and have not been studied in detail; they may therefore introduce biases into the resulting data: For example, [24] uses a process that consecutively augments triangles with neighboring triangles. This growth process necessarily stops at the outer edges of the triangulation, making them more likely to be part of a cell boundary than inner edges. The usage of these ad hoc models clearly indicates the need for models of random abstract cell complexes.

B Example Run on Toy Graph

This section provides an example run to give a better intuition on how the algorithm and its optimizations work. We will be using the following graph drawn from Erdős–Rényi ($n = 8, p = 0.5$):

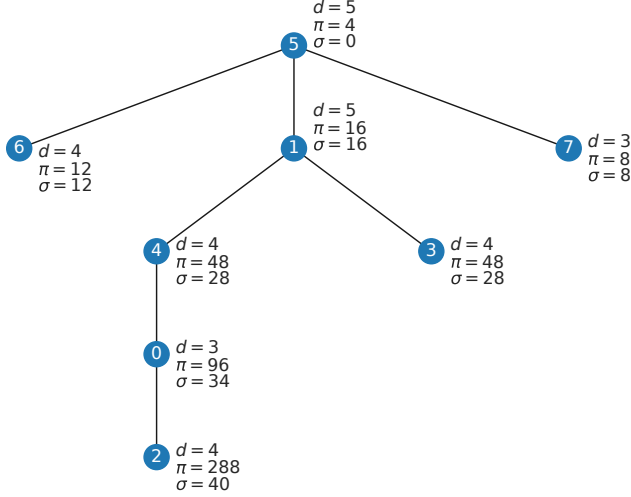


First, we sample a uniform spanning tree (left: highlighted on graph, right: displayed as rooted spanning tree).



To evaluate the occurrence probability of $\tilde{\rho}$ for all $c \in C_T$, we will iterate over all edges not in T .

First, we calculate $\sigma(r, u), \pi(r, u)$ for all $u \in V$ using the degrees:



Then, we calculate all lowest common ancestors using Tarjan's off-line lca algorithm [22]. In our example, we will look at the edge $(0, 3)$ with $\text{lca}(0, 3) = 1$. The corresponding cycle is $c = (0, 3, 1, 4)$.

As above, let $\gamma(n, p, l)$ denote the parts of the equation that do not depend on any degrees of specific nodes. Recall that:

$$\tilde{\rho}_c = \frac{\sum_{(u,v) \in c} (d(v) - 1)(d(v') - 1)}{\prod_{w \in c} d(w) - 1} \gamma(n, p, l) \quad (11)$$

$$= \frac{2 \cdot 3 + 3 \cdot 4 + 4 \cdot 3 + 3 \cdot 2}{2 \cdot 3 \cdot 4 \cdot 3} \gamma(n, p, l) = \frac{36}{72} \gamma(n, p, l) \quad (12)$$

We can calculate this in constant time from the partials π, σ along the tree and the degrees of u and v :

$$\sigma(0, 3) = \sigma(r, 0) + \sigma(r, 3) - 2\sigma(r, \text{lca}(0, 3)) = 34 + 28 - 2 \cdot 16 = 30$$

$$\pi(0, 3) = \frac{\pi(r, 0)\pi(r, 3)(d(\text{lca}(0, 3)) - 1)}{\pi(r, \text{lca}(0, 3))^2} = \frac{96 \cdot 48 \cdot 4}{16^2} = 72$$

$$\tilde{\rho}_c = \frac{\sigma(0, 3) + (d(0) - 1)(d(3) - 1)}{\pi(0, 3)} \gamma(n, p, l) = \frac{30 + 3 \cdot 2}{72} \gamma(n, p, l) = \frac{36}{72} \gamma(n, p, l) \quad \square$$

C Approximation of the occurrence probability ρ_c

A cycle is induced by a spanning tree if and only if all but one of its edges are part of a spanning tree. These edges then form a path on the spanning tree. To estimate the occurrence probability of a cycle, we can add the probabilities of each of these possible paths being included in a uniform spanning tree.

In the following, we introduce the Laplacian Random Walk, which provides us with another way to model the distribution of paths on the graph. From this, we derive an exact formula to calculate the occurrence probability ρ_c , and approximate this formula using the assumption that the graph was drawn from Erdős–Rényi.

C.1 The Laplacian Random Walk

For any simple (non-closed) path from u to v , the probability of all edges being part of a uniform spanning tree is the same probability as that of a Loop-Erased Random Walk (LERW), which is in turn the same as the Laplacian Random Walk (LRW) [19] from u to v taking that path [39].

A LERW starts at u and randomly selects a neighbor until reaching v . However, whenever a previously visited node w is reached, this loop is *erased*, i.e., all nodes visited since the last visit to w are removed from the resulting walk. Note that, in practice, uniform spanning trees are usually sampled using LERWs by Wilson’s algorithm [18].

The LRW achieves the same probability distribution as the LERW by avoiding loops in the first place. To do this, the transition probabilities have to be adjusted to account for the possibility of creating a loop before reaching the target node v . First, nodes that were already visited are never chosen. Second, nodes with no connection to the target node (except through the current node or previously visited nodes) are also never chosen as the LERW would have to return to a visited node before reaching the target node.

In every step of the LRW, the set of already visited nodes changes, thus necessitating a recalculation of these probabilities. The probabilities can be modeled using the Graph Laplace operator $L = D - A$: In each step i , Laplacian random walk defines a function $f_i : V \rightarrow \mathbb{R}$ on the nodes. For the target node v , it has a fixed value of $f_i(v) = 1$. Conversely, all nodes w already visited at time i have a fixed value of $f_i(w) = 0$. For all other nodes w , the probabilities are the solution to the laplace equation $L(f_i)(w) = 0$ holds. The probability to transition from u to w is then $\tau^{(i)}(w) = f_i(w) / \sum_{x \in \text{Neigh}(u)} f_i(x)$.

C.2 Estimating the occurrence probability

A spanning tree induces a cycle c if and only if all but one edge of c are part of the tree. The probability of each of these paths being part of the tree can be calculated using the laplacian random walk: For every edge (u, v) in c , we calculate the LRW probability of the path $c \setminus \{(u, v)\}$.

$$\rho_c = \sum_{(u,v) \in c} \prod_{(w,x) \in c \setminus \{(u,v)\}} p_i(w) = \sum_{(u,v) \in c} \prod_{(w,x) \in c \setminus \{(u,v)\}} \frac{f_i(x)}{\sum_{y \in \text{Neigh}(w)} f_i(y)} \quad (13)$$

Since the LRW requires calculating f_i for every step of the walk, it is too computationally expensive for our purpose. To efficiently approximate this, we use the expected graph for our calculations. The expected ER graph is a weighted complete graph with a weight of p on each edge. Since all nodes that have not been visited and are not v are symmetric (including weights), their \tilde{f}_i will be the same, meaning only the number of visited nodes i and x influence this. This gives us the following estimation:

$$\forall u : f_i(u) \approx \begin{cases} 1 & \text{if } u \text{ is the target} \\ 0 & \text{if } u \text{ has been visited} \\ \tilde{f}_i := \frac{i \cdot 0 + 1 \cdot 1}{i+1} = \frac{1}{i+1} & \text{else} \end{cases} \quad (14)$$

We denote the transition probability of the laplacian random walk in step i by $\tau_c^{(i)}$. For the first step, no other node has been visited and all neighbors are either unvisited or v . Out of the $n - 1$ neighbors in the expected graph, $n - 2$ are unvisited with $f_i \approx \tilde{f}_i$, and one is the target node.

$$\tilde{\tau}_c^{(1)} = \frac{\tilde{f}_i}{d(w) \left(\frac{n-2}{n-1} \tilde{f}_i + \frac{1}{n-1} \right)} \quad (15)$$

$$= \frac{\frac{1}{2}}{d(w) \frac{1}{n-1} \left(\frac{n-2}{2} + 1 \right)} \quad (16)$$

$$= \frac{n-1}{d(w) (n-2+2)} \quad (17)$$

$$= \frac{1}{d(w)} \frac{n-1}{n} \quad (18)$$

After step 1: Note that we already know that one neighbor has been visited in the previous step, so we only need to consider the remaining $d(w) - 1$ neighbors. Of these, in expectation, $\frac{i-2}{n-2}$ have been visited so far and $\frac{1}{n-2}$ neighbors are the target node v . $\frac{n-i-1}{n-2}$ are unvisited.

$$\tilde{\tau}_c^{(i)} = \frac{\tilde{f}_i}{(d(w) - 1) \frac{1}{n-2} ((n-i-1) \tilde{f}_i + 1)} \quad (19)$$

$$= \frac{1}{d(w) - 1} \frac{(n-2) \frac{1}{i+1}}{\frac{n-i-1}{i+1} + 1} \quad (20)$$

$$= \frac{1}{d(w) - 1} \frac{n-2}{n-i-1+i+1} \quad (21)$$

$$= \frac{1}{d(w) - 1} \frac{n-2}{n} \quad (22)$$

For the transition to v (step $l-1$), we know that v is a neighbor. Therefore, there is one neighbor that was certainly visited, one that has value 1, and of the remaining $d(w) - 2$ neighbors, $\frac{n-(l-1)-1}{n-3} = \frac{n-l}{n-3}$ have not been visited and have value f_{l-1} :

$$\tilde{\tau}_c^{(l-1)} = \frac{1}{1 + (d(w) - 2) \frac{n-l}{n-3} f_{l-1}} \quad (23)$$

$$= \frac{1}{1 + \frac{(d(w)-2) \frac{n-l}{l}}{n-3}} \quad (24)$$

$$\approx \frac{1}{1 + \frac{(n-1) \frac{n-l}{l}}{n-3}} =: \tilde{\tau}_c^{(l-1)} \quad (25)$$

cycle length is $l+1$, path is l ; $(u, v) \in c$ denotes edges

$$\rho_c \approx \sum_{(u,v) \in c} \tilde{\tau}_c^{(l-1)} \tilde{\tau}_c^{(1)} \prod_{i=2}^{l-2} \tilde{\tau}_c^{(i)} \quad (26)$$

$$= \sum_{(u,v) \in c} \tilde{\tau}_c^{(l-1)} \tilde{\tau}_c^{(1)} (d(v') - 1) \prod_{w \in c, u \neq w \neq v} \frac{1}{d(w) - 1} \frac{n-2}{n} \quad (27)$$

$$= \frac{\sum_{(u,v) \in c} \tilde{\tau}_c^{(l-1)} \frac{d(u)-1}{d(u)} \frac{n-1}{n} (d(v) - 1)(d(v') - 1)}{\prod_{w \in c} d(w) - 1} \cdot \left(\frac{n-2}{n} \right)^{l-3} \quad (28)$$

$$= \frac{\sum_{(u,v) \in c} \tilde{\tau}_c^{(l-1)} \frac{d(u)-1}{d(u)} (d(v) - 1)(d(v') - 1)}{\prod_{w \in c} d(w) - 1} \cdot \left(\frac{n-2}{n} \right)^{l-3} \frac{n-1}{n} \quad (29)$$

$$\approx \frac{\sum_{(u,v) \in c} \tilde{\tau}_c^{(l-1)} (d(v) - 1)(d(v') - 1)}{\prod_{w \in c} d(w) - 1} \cdot \left(\frac{n-2}{n} \right)^{l-3} \frac{n-1}{n} \frac{(n-1)q-1}{(n-1)q} =: \tilde{\rho}_c \quad (30)$$

Note that we approximated $\frac{d(u)-1}{d(u)} \approx \frac{(n-1)q-1}{(n-1)q}$ as this makes it easier to compute. By substituting $\tilde{\tau}_c^{(l-1)}$ for $\tilde{\tau}_c^{(l-1)}$, we arrive at:

$$\tilde{\rho}_c := \frac{\sum_{(u,v) \in c} \tilde{\tau}_c^{(l-1)} (d(v) - 1)(d(v') - 1)}{\prod_{w \in c} d(w) - 1} \cdot \left(\frac{n-2}{n} \right)^{l-3} \frac{n-1}{n} \frac{(n-1)q-1}{(n-1)q} \quad (31)$$

$$= \frac{\sum_{(u,v) \in c} (d(v) - 1)(d(v') - 1)}{\prod_{w \in c} d(w) - 1} \cdot \left(\frac{n-2}{n} \right)^{l-3} \frac{n-1}{n} \frac{(n-1)q-1}{(n-1)q} \tilde{\tau}_c^{(l-1)} \quad (32)$$

D Additional Plots

The evaluation code used to generate these plots is available at github.com/josefhoppe/random-abstract-cell-complexes.

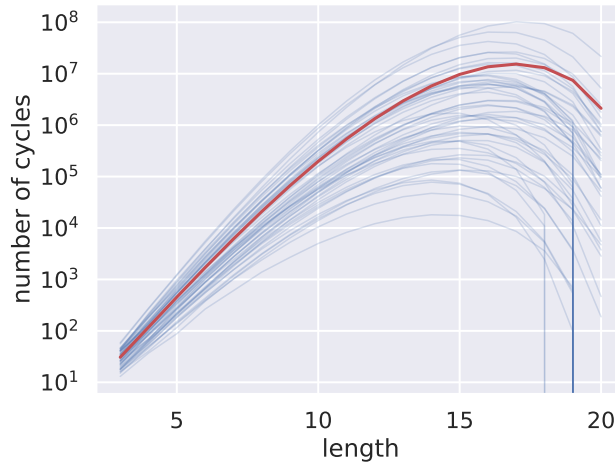


Figure 9: Number of simple cycles N_l on 50 graphs sampled from Erdős–Rényi with $n = 20$, $p = 0.3$. The red line indicates the a priori estimation \mathcal{N}_l . There is a large variance in the number of cells for a given l , especially as $l \rightarrow n$.

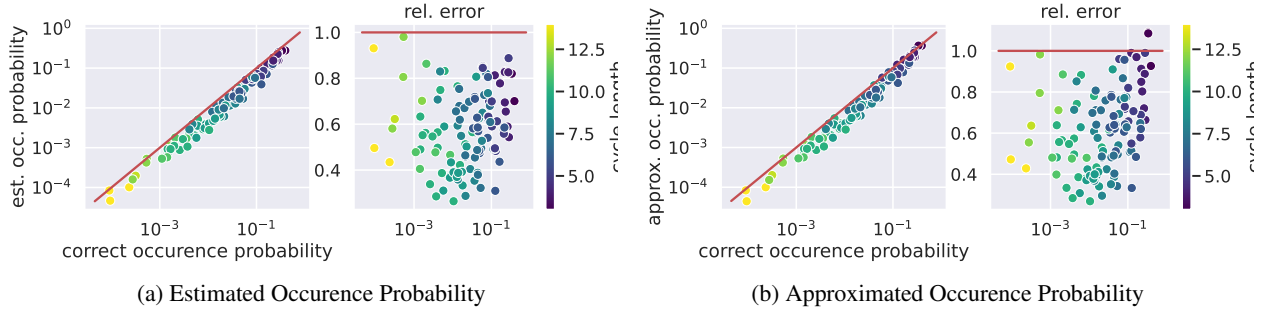
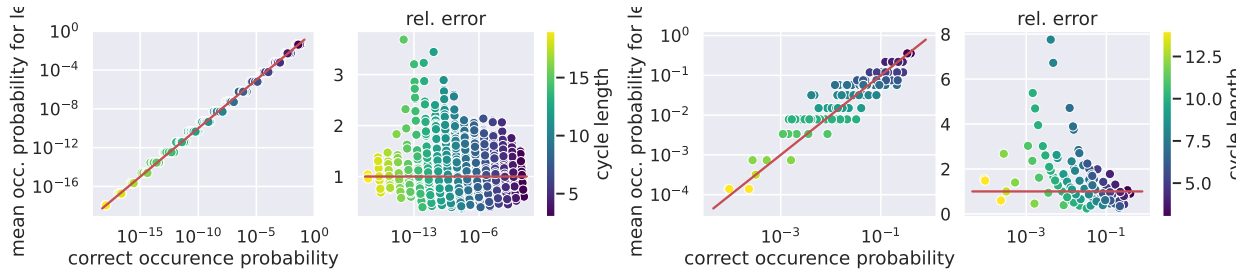


Figure 10: The estimated (a) and approximated (b) probability of simple cycles to be induced by a random spanning tree on one graph sampled from ER with $n = 30, p = 0.1$; cycles for evaluation obtained from 10 random STs. Both methods are less accurate than for $p = 0.5$ (comp. Figure 6), which is expected as the connectedness decreases and relative variance in degree increases (i.e., the graph is much less similar to the expected graph in behavior). Even with these challenges, the error is still less than one order of magnitude.



(a) Evaluation on the same cycles and graph sampled from ER with $n = 30, p = 0.5$ as Figure 6. (b) Evaluation on the same cycles and graph sampled from ER with $n = 30, p = 0.1$ as Figure 10.

Figure 11: The approximation error of a hypothetical approximation that assigns each cycle the mean probability of all cycles with the same length, for a moderate configuration (a) and a sparse configuration (b). The estimation error is significantly larger than either of our approaches, i.e., our approaches detect significantly more than just the cycle length.

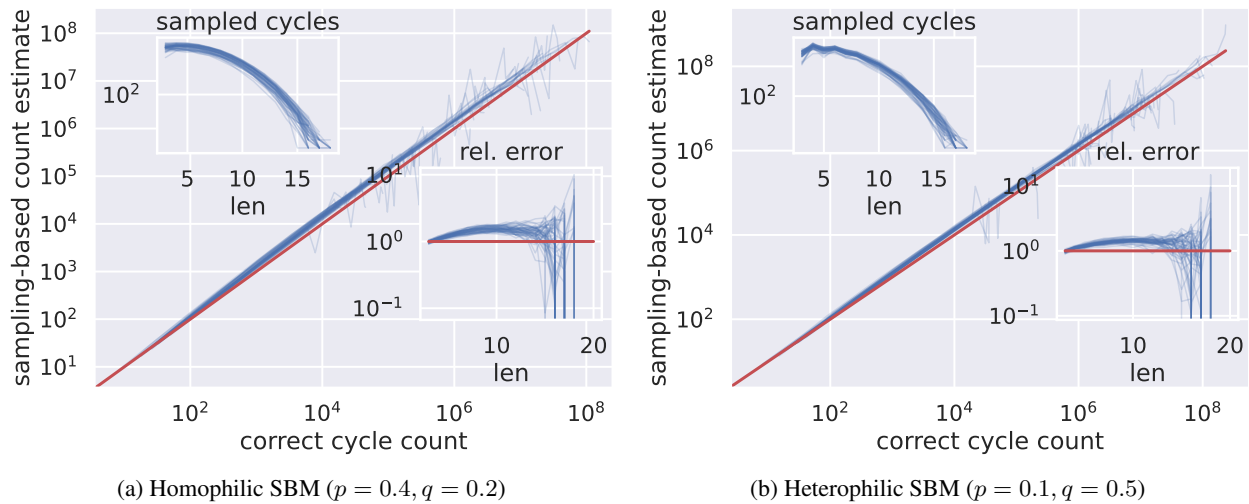


Figure 12: The estimated number of cycles for different lengths, number of sampled cells, and relative error by length on 50 graphs sampled from a homophilic (a) and heterophilic (b) SBM, each with two blocks of 10 nodes. In both cases, the accuracy is surprisingly good considering that the approximations assume an underlying ER-Graph. The accuracy is massively reduced for lengths where the sampled number of cells is too small.

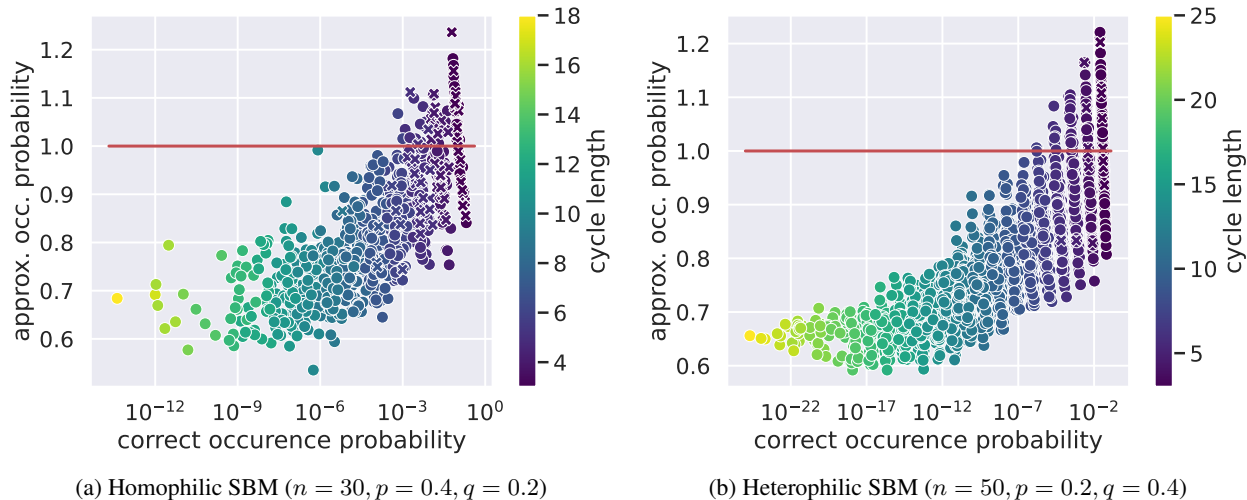


Figure 13: The approximated occurrence probability (relative to the correct probability) for cycles on graphs sampled from the SBM. Xs mark cycles that only include nodes from one block.

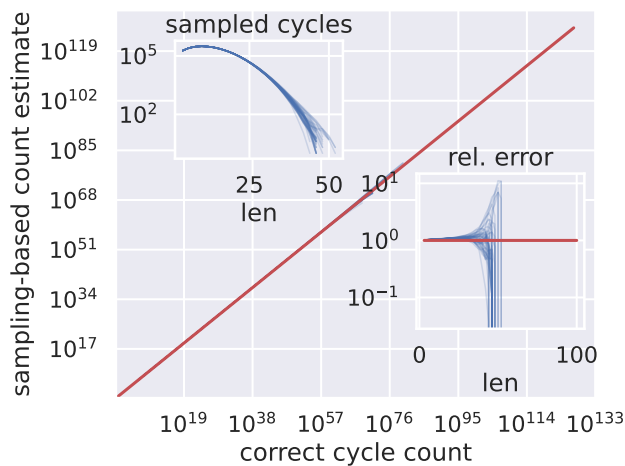


Figure 14: The sampling-based estimation on $K_{50,50}$

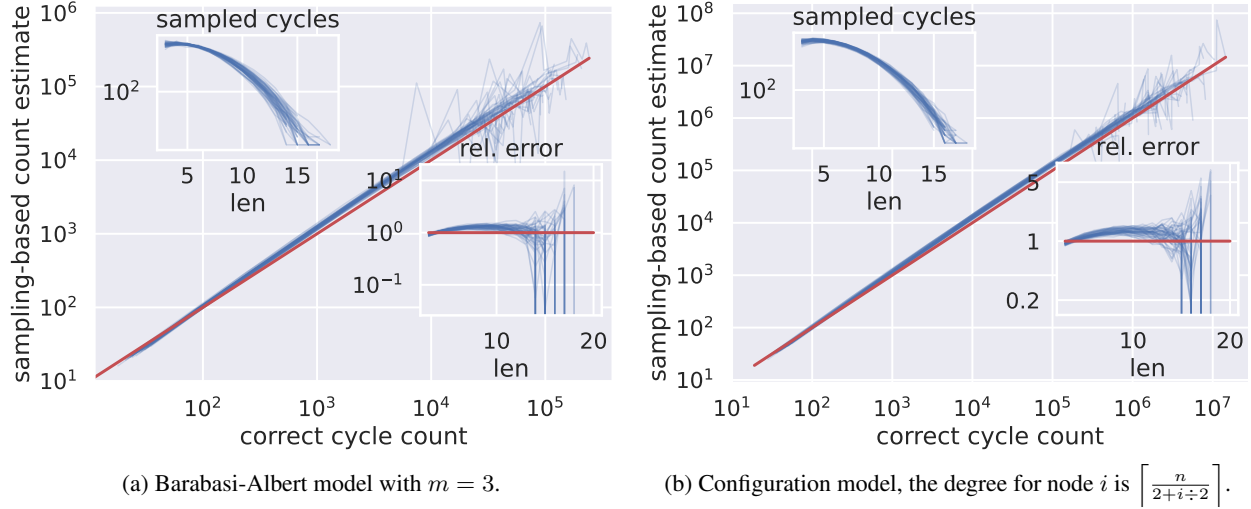


Figure 15: The sampling-based estimation on graphs sampled from random graph models with uneven degree distributions (50 graphs with $n = 20$ nodes each). While the error increases further in both cases, it is still significantly more accurate than expected.

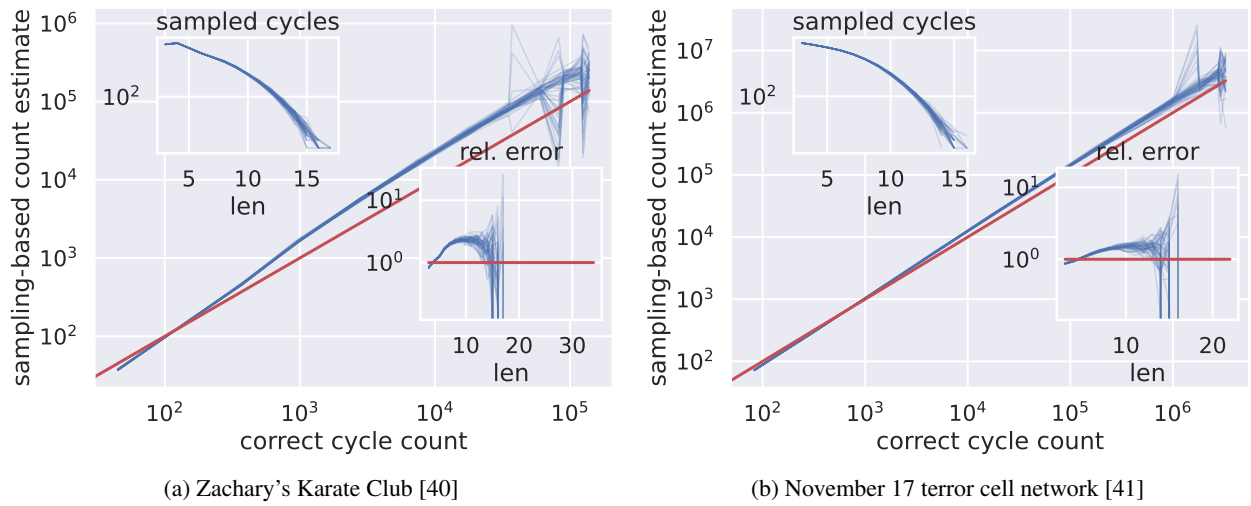


Figure 16: The estimated number of cycles for different lengths, number of sampled cycles, and relative error by length on 50 runs sampled on two real-world graphs. In both cases — given a reasonable number of occurring cycles — the estimation error is within an order of magnitude, but the karate club shows a significantly larger error. Given its very much non-ER-like structure, this is to be expected.

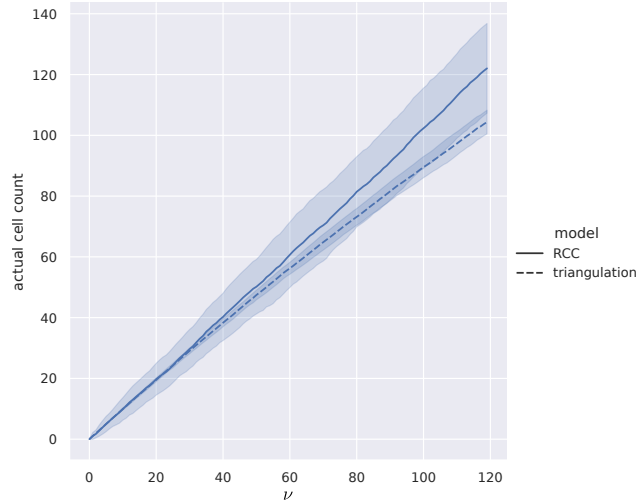


Figure 17: The actual number of cells is, in expectation, ν .

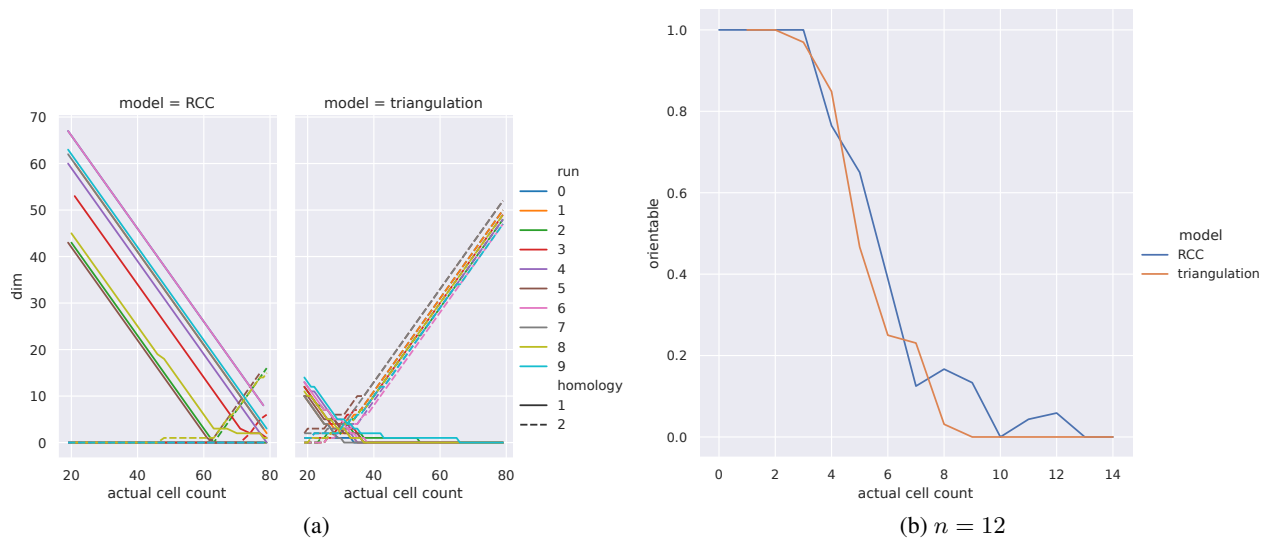


Figure 18: Analysis of random cell complexes, comparing our model (RCC) to the triangulation-based model from [24] (triangulation). (a) compares the dimension of the 1- and 2-cohomology, showing that, in both models, 2-homologies are only rarely added significantly before all 2-cohomologies have been filled. (b) shows what fraction of sampled CCs is orientable, again showing a similar behavior for the two models.